

## Determination of the microstructure of Eu-treated ZnO nanowires by x-ray absorption

W. L. Huang, J. Labis, S. C. Ray, Y. R. Liang, C. W. Pao, H. M. Tsai, C. H. Du, W. F. Pong, J. W. Chiou, M.-H. Tsai, H. J. Lin, J. F. Lee, Y. T. Chou, J. L. Shen, C. W. Chen, and G. C. Chi

Citation: [Applied Physics Letters](#) **96**, 062112 (2010); doi: 10.1063/1.3304071

View online: <http://dx.doi.org/10.1063/1.3304071>

View Table of Contents: <http://scitation.aip.org/content/aip/journal/apl/96/6?ver=pdfcov>

Published by the [AIP Publishing](#)

---

### Articles you may be interested in

[Investigating the source of deep-level photoluminescence in ZnO nanorods using optically detected x-ray absorption spectroscopy](#)

J. Appl. Phys. **114**, 153517 (2013); 10.1063/1.4824810

[Local lattice distortions in single Co-implanted ZnO nanowires](#)

Appl. Phys. Lett. **103**, 141911 (2013); 10.1063/1.4824117

[Characterization of lattice defects by x-ray absorption spectroscopy at the Zn K-edge in ferromagnetic, pure ZnO films](#)

J. Appl. Phys. **110**, 063507 (2011); 10.1063/1.3631774

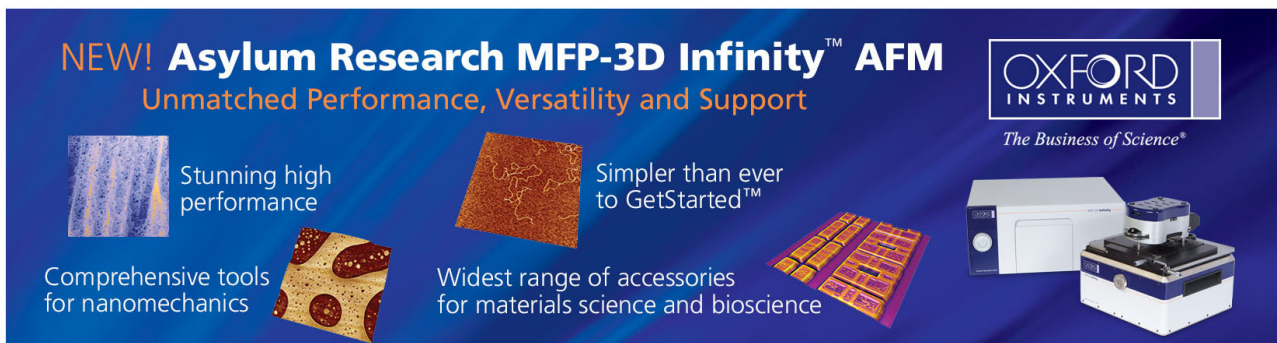
[X-ray absorption and magnetic circular dichroism characterizations of Mn doped ZnO](#)

Appl. Phys. Lett. **91**, 162503 (2007); 10.1063/1.2794764

[Diameter dependence of the electronic structure of ZnO nanorods determined by x-ray absorption spectroscopy and scanning photoelectron microscopy](#)

Appl. Phys. Lett. **85**, 3220 (2004); 10.1063/1.1802373

---

The advertisement features a dark blue background with a grid of images showing various AFM scan results. The text 'NEW! Asylum Research MFP-3D Infinity™ AFM' is prominently displayed in white and orange. Below it, the slogan 'Unmatched Performance, Versatility and Support' is written in orange. The Oxford Instruments logo, 'The Business of Science®', is in the top right. Four key features are listed: 'Stunning high performance' (with a scan image), 'Simpler than ever to GetStarted™' (with a scan image), 'Comprehensive tools for nanomechanics' (with a scan image), and 'Widest range of accessories for materials science and bioscience' (with a scan image). An image of the MFP-3D Infinity AFM system is shown in the bottom right corner.

## Determination of the microstructure of Eu-treated ZnO nanowires by x-ray absorption

W. L. Huang,<sup>1</sup> J. Labis,<sup>1,a)</sup> S. C. Ray,<sup>1,2</sup> Y. R. Liang,<sup>1</sup> C. W. Pao,<sup>1</sup> H. M. Tsai,<sup>1</sup> C. H. Du,<sup>1</sup> W. F. Pong,<sup>1,b)</sup> J. W. Chiou,<sup>3</sup> M.-H. Tsai,<sup>4</sup> H. J. Lin,<sup>5</sup> J. F. Lee,<sup>5</sup> Y. T. Chou,<sup>6</sup> J. L. Shen,<sup>6</sup> C. W. Chen,<sup>7</sup> and G. C. Chi<sup>8</sup>

<sup>1</sup>Department of Physics, Tamkang University, Tamsui 251, Taiwan

<sup>2</sup>School of Physics, University of the Witwatersrand, Private Bag 3, WITS 2050, Johannesburg, South Africa

<sup>3</sup>Department of Applied Physics, National University of Kaohsiung, Kaohsiung 811, Taiwan

<sup>4</sup>Department of Physics, National Sun Yat-Sen University, Kaohsiung 804, Taiwan

<sup>5</sup>National Synchrotron Radiation Research Center, Hsinchu 300, Taiwan

<sup>6</sup>Department of Physics, Chung Yuan Christian University, Chungli 320, Taiwan

<sup>7</sup>Department of Physics, National Central University, Chungli 320, Taiwan

<sup>8</sup>Department of Photonics, National Chiao Tung University, Hsinchu 300, Taiwan

(Received 7 December 2009; accepted 12 January 2010; published online 9 February 2010)

X-ray absorption near-edge structure (XANES), extended x-ray absorption fine structures (EXAFS), and photoluminescence measurements were used to elucidate the microstructural and photoluminescence properties of ZnO nanowires (ZnO-NWs) that had been treated with Eu by thermal diffusion. The O *K*- and Eu *L*<sub>3</sub>-edge XANES and EXAFS spectra at the Zn *K*- and Eu *L*<sub>3</sub>-edge verified the formation of Eu<sub>2</sub>O<sub>3</sub>-like layer on the surface of ZnO-NWs. X-ray diffraction, XANES and EXAFS measurements consistently suggest the lack of substitutional doping of Eu ions at the Zn ion sites in the interior of ZnO-NWs. The clear sharp and intense emission bands in the range 610–630 nm of Eu-treated ZnO-NWs originated from the intra-4*f* transition of Eu ions in the Eu<sub>2</sub>O<sub>3</sub>-like surface layer. © 2010 American Institute of Physics. [doi:10.1063/1.3304071]

Zinc oxide (ZnO) is a well-known wide band-gap semiconductor with a large exciton binding energy at room temperature. It has attracted much interest in recent years because of its unique properties and potential applications.<sup>1–3</sup> Recent studies of this material have focused on its applications in optoelectronics and light-emitting devices. ZnO emits over a wide range of the visible spectrum and UV luminescence. Many studies of rare-earth (RE)-treated ZnO and RE-induced changes in their optical properties have tended to conclude that trivalent RE ions are effective luminescence centers.<sup>4–7</sup> The results of these studies have also suggested that energy can be transferred from the ZnO matrix to Eu activator ions, yielding narrow and intense emission lines that are associated with 4*f* intrashell transitions. However, the direct transfer of energy from ZnO to Eu ions has been argued to be unfeasible, because the lifetime of the exciton in ZnO is much shorter than the time required for energy transfer,<sup>8</sup> the difference between ionic radii (Eu<sup>3+</sup> ion: ~0.95 Å and Zn<sup>2+</sup> ion: ~0.74 Å) is large, and the charges of Eu<sup>3+</sup> and Zn<sup>2+</sup> ions do not balance.<sup>9</sup> Eu ions can be incorporated into a ZnO lattice with a nanostructure by the formation of surface defects,<sup>10,11</sup> and substituted in the lattice or localized at the grain boundaries,<sup>12,13</sup> which serve as energy traps and support the transfer of energy in the system. However, direct microstructural evidence of the effect of Eu ions on the photoluminescence (PL) of Eu-treated ZnO matrix is lacking. Therefore, an understanding of the mechanism of energy transfer between the ZnO matrix and Eu ions as a cause of light emission and the enhancement of emission is

very valuable. In particular, the relationship between the PL property and the electronic/atomic structures of Eu-treated ZnO nanowires (ZnO-NWs) is very important. In this letter, x-ray diffraction (XRD), PL, x-ray absorption near-edge structure (XANES), and extended x-ray absorption fine structure (EXAFS) are measured to address the above issues.

The XANES and EXAFS measurements were carried out at the National Synchrotron Radiation Research Center in Hsinchu, Taiwan. Pure ZnO-NWs were grown by chemical vapor deposition, Eu-treated ZnO-NWs were obtained by thermal diffusion of Eu atoms into ZnO-NWs. Commercial-grade Eu oxide (Eu<sub>2</sub>O<sub>3</sub>) powder was compared with the samples. The diameter of ZnO-NWs was approximately 200 nm; they were approximately 1 μm long. Details of the preparation of Eu-treated ZnO-NWs and ZnO-NWs can be found elsewhere.<sup>11</sup>

Figure 1 presents XRD patterns of Eu-treated and untreated ZnO-NWs along with that of reference Eu<sub>2</sub>O<sub>3</sub>. All peaks in the XRD patterns of Eu-treated and untreated ZnO-NWs can be indexed to (hexagonal) wurtzite-phase ZnO. No diffraction peak from Eu<sub>2</sub>O<sub>3</sub> or another Eu-impurity was observed, suggesting that either Eu ions were substituted at the Zn ion sites in ZnO-NWs or formed a very small/thin Eu-oxide layer on the surface, which layer was too thin to be detected by XRD. When Eu ions randomly substitute for Zn ions, diffraction peaks are expected to shift toward smaller angles, since the radius of Eu<sup>3+</sup> (0.95 Å) exceeds that of Zn<sup>2+</sup> (0.74 Å), such that the substitution increases the interplane distance. However, the XRD data in Fig. 1 do not reveal any diffraction peak shift, seemingly excluding the possibility of substitutional doping by Eu ions at the Zn ion sites in the interior of Eu-treated ZnO-NWs. The high-resolution transmission electron microscopy (HR-TEM) image in inset (a) in Fig. 1 reveals sharp and clear ordered-lattices in ZnO-NWs.

<sup>a)</sup>Also at permanent address: Department of Physics, College of Science, MSU-General Santos City, Philippines.

<sup>b)</sup>Author to whom correspondence should be addressed. Electronic mail: wfpong@mail.tku.edu.tw.

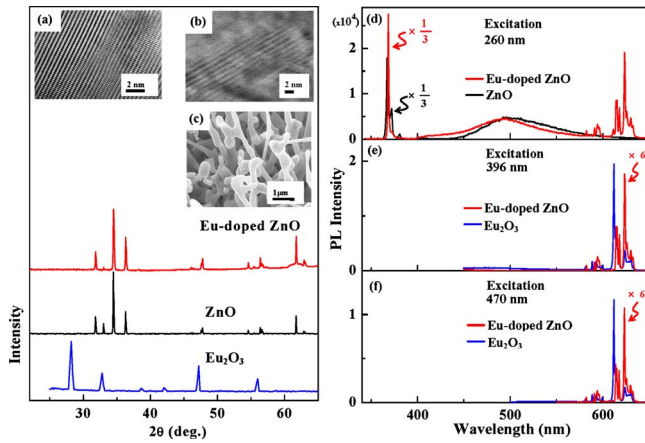


FIG. 1. (Color online) XRD patterns of Eu-treated ZnO-NWs, ZnO-NWs and reference  $\text{Eu}_2\text{O}_3$  powder. Insets [(a)–(c)] present, respectively, HR-TEM images of ZnO-NWs and Eu-treated ZnO-NWs, and SEM image of Eu-treated ZnO-NWs. Panels [(d)–(f)] present PL spectra of Eu-treated ZnO-NWs, ZnO-NWs, and  $\text{Eu}_2\text{O}_3$  under different light excitations at 15 K.

In contrast, the HR-TEM image in inset (b) displays relatively oblique and disordered lattices in Eu-treated ZnO-NWs, attributable to the presence of Eu-oxide on the surface.<sup>11</sup> The scanning electron microscopic (SEM) image in inset (c) shows the round structure of Eu-treated ZnO-NWs and their overall growth in the upright/vertical direction associated with the thermal diffusion of Eu atoms. Panels [(d)–(f)] in Fig. 1 present the PL spectra of Eu-treated ZnO-NWs under excitation by 260 (4.77 eV), 396 (3.13 eV), and 470 (2.64 eV) nm He-Ar laser light at 15 K. The figure reveals strong near-band-edge emission at  $\sim 370$  nm (3.3 eV). Corresponding green luminescence is centered at  $\sim 500$  nm [panel (d)] and sharp and intense emissions are observed in the spectra in the range 610–630 nm [panels (d)–(f)] under the three excitations. The broad green luminescence in panel (d) has been suggested to be caused by vacancy defects.<sup>5,14</sup> The shift in the broad green luminescence of Eu-treated ZnO-NWs relative to that of ZnO-NWs is attributable to deep trapped hole states in oxygen vacancies and excess oxygen on the surface of NWs.<sup>14</sup> Panels (d)–(f) also present the PL spectra of ZnO-NWs and  $\text{Eu}_2\text{O}_3$  under various excitations at 15 K for comparison. Clearly, the excitation energies at 396 (3.13 eV) and 470 nm (2.64 eV) are lower than the band gap of pure ZnO-NWs ( $\sim 3.4$  eV).<sup>15</sup> The sharp and intense emissions in the range 610–630 nm from Eu-treated ZnO-NWs under various excitations suggest that Eu ions may gain energy from ZnO-NWs, giving rise to an intra- $4f$  transition.<sup>4–7</sup> The emissions in the range 610–630 nm of Eu-treated ZnO-NWs are similar to those of the reference  $\text{Eu}_2\text{O}_3$ , as shown in panels (e) and (f) in Fig. 1. Careful observation reveals that, in spite of discernible similarity, the Stark splitting in the spectra are still somewhat different, which can be explained by the highly defective nature of the produced  $\text{Eu}_2\text{O}_3$ -like layer that covers the surface. The formation of other compounds, such as  $\text{ZnEu}_2\text{O}_4$ , which has been reported to be a stable oxide,<sup>16</sup> could also be a possibility, although the analysis of the data in the present work shows that the  $\text{Eu}_2\text{O}_3$ -like layer is most likely.

Figure 2 presents normalized O  $K$ -edge XANES spectra of Eu-treated, untreated ZnO-NWs, and reference  $\text{Eu}_2\text{O}_3$ . The characteristic features  $A_1$ – $E_1$  in the O  $K$ -edge spectrum of ZnO-NWs corresponds primarily to O  $1s$  transitions to the

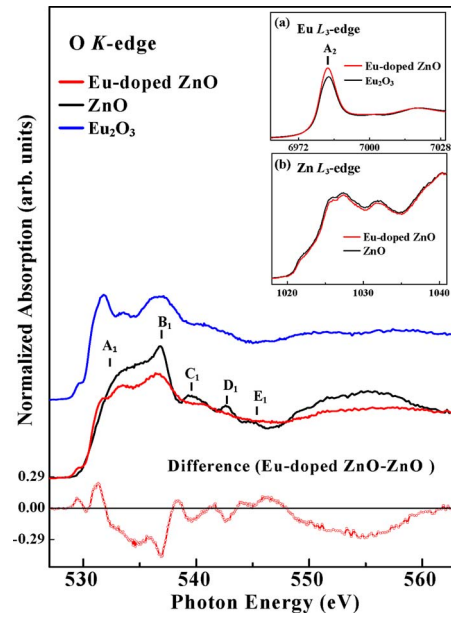


FIG. 2. (Color online) Normalized O  $K$ -edge XANES spectra of Eu-treated ZnO-NWs, ZnO-NWs and  $\text{Eu}_2\text{O}_3$  powder. Lower inset plots difference XANES spectrum between Eu-treated ZnO-NWs and ZnO-NWs. Insets (a) and (b) present, respectively, Eu  $L_3$ -edge XANES of Eu-treated ZnO-NWs and  $\text{Eu}_2\text{O}_3$ , and Zn  $L_3$ -edge XANES of Eu-treated ZnO-NWs and ZnO-NWs.

O  $2p_{ab}$  (along the bilayer) and O  $2p_c$  (along the  $c$ -axis) unoccupied states.<sup>15,17</sup> The lower panel in Fig. 2 presents the difference spectrum between Eu-treated and untreated ZnO-NWs. The overall spectral intensity of Eu-treated ZnO-NWs is reduced and the near-edge feature is broadened relative to those of ZnO-NWs, indicating that the number of O  $2p$  unoccupied states decreases following the Eu-diffusion process, suggesting an increase in the occupation of the O  $2p$  orbitals and in the negative effective charge of the O ion. The increase in the effective charge of the O ions is explained by the fact that the Pauling's electronegativity of Eu (1.2) is much smaller than that of Zn (1.65).<sup>18</sup> The inset (a) in Fig. 2 displays XANES spectra at the Eu  $L_3$ -edge of the Eu-treated ZnO-NWs and  $\text{Eu}_2\text{O}_3$ . The Eu-treated ZnO-NWs and  $\text{Eu}_2\text{O}_3$  yield almost identical spectral line-shapes with a strong feature ( $A_2$ ) at the same energy threshold,  $\sim 6983.7$  eV, clearly suggesting the formation by trivalent Eu ions of an  $\text{Eu}_2\text{O}_3$ -like layer on the surface, rather than the substitution of Zn ions in the interior of the NWs. Feature  $A_2$  of Eu-treated ZnO-NWs corresponds to the transition of Eu  $2p$  to  $5d$  unoccupied states and is considerably more intense than that of reference  $\text{Eu}_2\text{O}_3$ . The relatively high intensity of feature  $A_2$  may be caused by the enhancement of the localization of Eu  $5d$  states in Eu-treated ZnO-NWs associated with the reduced size of NWs. The enhanced feature  $A_2$  is also consistent with the fact that the overall intensity of spectral features in Zn  $L_3$ -edge XANES, which corresponds to Zn  $2p$  to  $4s/3d$  transitions in Eu-treated ZnO-NWs, is slightly lower than the intensity of that of ZnO-NWs, as shown in the inset (b) in Fig. 2.

Figure 3 and insets (a) and (b) in Fig. 3 present the amplitude of the Fourier transform (FT) obtained from the EXAFS  $k^3\chi$  data for Eu-treated ZnO-NWs, untreated ZnO-NWs and  $\text{Eu}_2\text{O}_3$ , and their corresponding oscillations at the Zn  $K$ -edge and Eu  $L_3$ -edge at an angle of incidence  $\theta = 37^\circ$ . The first and second main features in the FT spectra at the Zn  $K$ -edge of ZnO-NWs correspond to the nearest-neighbor

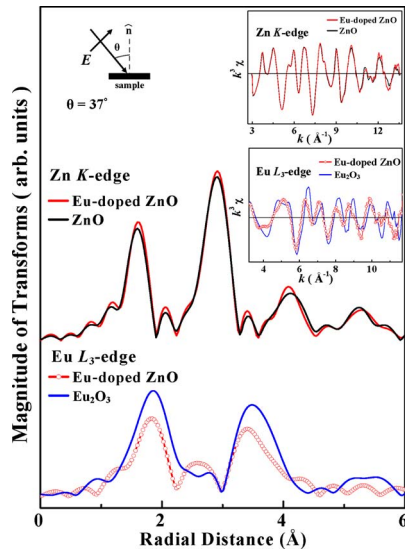


FIG. 3. (Color online) FT of EXAFS  $k^3\chi$  data from  $k=3.2$  to  $13.5$  Å<sup>-1</sup> at Zn  $K$ -edge of Eu-treated ZnO-NWs, and ZnO-NWs, and Eu  $L_3$ -edge from  $k=3.2$  to  $10.5$  Å<sup>-1</sup> of Eu-treated ZnO-NWs and  $\text{Eu}_2\text{O}_3$  powder, respectively. Upper left part of inset presents experimental geometry, where  $E$  is the polarization of the incoming photons, and  $\theta(=37^\circ)$  is the angle of incidence. Upper right-inset presents the Zn  $K$ -edge EXAFS  $k^3\chi$  data of Eu-treated ZnO-NWs and ZnO-NWs. Lower right-inset shows Eu  $L_3$ -edge EXAFS  $k^3\chi$  data of Eu-treated ZnO-NWs and  $\text{Eu}_2\text{O}_3$ .

(NN) Zn-O and the next-nearest-neighbor (NNN) Zn-Zn bond lengths. Clearly, the line-shapes and the radial distribution of the FT spectra at the Zn  $K$ -edge of the Eu-treated ZnO-NWs are nearly identical to those of ZnO-NWs but the overall spectral intensities of the NN and NNN features are slightly higher. These results suggest the following. (i) Eu atoms in the thermal diffusion process did not substitute for host Zn ions in Eu-treated ZnO-NWs, because if the Eu atoms had randomly substituted Zn ions in the interior of the NWs, the local atomic structure at the Zn sites should be strongly distorted, due to the large difference between the ionic radii of  $\text{Eu}^{3+}$  and  $\text{Zn}^{2+}$ , and such distortion was not observed. The XRD data are consistent with this finding. (ii) Most of the Eu atoms substituted at the Zn sites on the surface layer and formed a stable  $\text{Eu}_2\text{O}_3$ -like layer, such that Zn ions with dangling bonds or defects, which have a larger degree of disorder, were depleted. This argument explains why the spectral intensities of the NN and NNN features in the FT spectra of Eu-treated ZnO-NWs slightly exceed those in the spectra of ZnO-NWs. The FT at the Eu  $L_3$ -edge of Eu-treated ZnO-NWs and  $\text{Eu}_2\text{O}_3$  presented in the lower part of Fig. 3 supports this argument. Clearly, the general line-shape and the radial distribution of the Eu  $L_3$ -edge FT spectra of Eu-treated ZnO-NWs are similar to those of reference  $\text{Eu}_2\text{O}_3$ , indicating that the local atomic structure of Eu ions in Eu-treated ZnO-NWs is similar to that of  $\text{Eu}_2\text{O}_3$ . The lower intensities of the NN and NNN features in the FT spectra of the Eu-treated ZnO-NWs reveal that the structural distortion of Eu-treated ZnO-NWs exceeds that of  $\text{Eu}_2\text{O}_3$ , possibly because of an increase in the number of dangling bonds/surface states of the  $\text{Eu}_2\text{O}_3$ -like layer on the surface of ZnO-NWs.<sup>19</sup> Notably, the EXAFS FT spectra of the Eu  $L_3$ -edge of the Eu-treated ZnO-NWs clearly differ from those at the Zn  $K$ -edge, further indicating the lack of significant substitution of Zn ions by Eu ions in Eu-treated ZnO-NWs. Additionally, polarization-dependent EXAFS measure-

ments (not shown in the figure) at the Eu  $L_3$ -edge, with two angles of incidence,  $\theta=0^\circ$  (normal incidence) and  $70^\circ$  (grazing incidence), were also made. The spectral intensities of the NN and NNN features in the FT spectra at  $\theta=70^\circ$  are lower than those at  $\theta=0^\circ$ , suggesting greater surface sensitivity at the grazing incidence,  $\theta=70^\circ$ , which is associated with larger structural disorder, and leads to the detection of more dangling bonds or defects on the  $\text{Eu}_2\text{O}_3$ -like surface layer. This finding is evidence of the presence of an  $\text{Eu}_2\text{O}_3$ -like surface layer. If Eu ions had been incorporated at the interstitial sites of the grain boundaries in the ZnO-NWs matrix, polarization-dependent EXAFS measurements would differ negligible between the two incident angles.

As stated above, the enhancement of PL in Eu-treated ZnO-NWs is generally believed to involve the absorption of photon energy by Eu ions, causing their electrons to transition from the ground state to the excited state. This process may be associated with structural defects, chemical inhomogeneities, and oxygen vacancies formed by Eu. When ZnO-NWs absorb photon energy, electron-hole pairs are generated. Some of the energy that is released by the recombination of electron-hole pairs is transferred to Eu ions, so that they act as luminescence centers with  $4f$  intrashell transitions, yielding narrow and intense emission lines under indirect excitation.<sup>4-7</sup> However, earlier studies have also shown that the transfer of energy from the ZnO host to Eu ions is very inefficient in Eu-treated ZnO.<sup>4,20</sup> The measurements in this work demonstrate that the sharp and intense emission from Eu-treated ZnO-NWs originated at the Eu centers in the  $\text{Eu}_2\text{O}_3$ -like surface layer under direct light excitation.

<sup>1</sup>D. M. Bagnall, Y. F. Chen, Z. Zhu, T. Yao, S. Koyama, M. Y. Shen, and T. Goto, *Appl. Phys. Lett.* **70**, 2230 (1997).

<sup>2</sup>M. H. Huang, S. Mao, H. Feick, H. Yan, Y. Wu, H. Kind, E. Weber, R. Russo, and P. Yang, *Science* **292**, 1897 (2001).

<sup>3</sup>X. Wang, J. Song, and Z. L. Wang, *Science* **316**, 102 (2007).

<sup>4</sup>L. Armelao, G. Bottaro, M. Pascolini, M. Sessolo, E. Tondello, M. Bettinelli, and A. Speghini, *J. Phys. Chem. C* **112**, 4049 (2008).

<sup>5</sup>Y. Yu, Y. Wang, D. Chen, P. Huang, E. Ma, and F. Bao, *Nanotechnology* **19**, 055711 (2008).

<sup>6</sup>J. Bang, H. Yang, and P. H. Holloway, *J. Chem. Phys.* **123**, 084709 (2005).

<sup>7</sup>A. Ishizumi and Y. Kanemitsu, *Appl. Phys. Lett.* **86**, 253106 (2005).

<sup>8</sup>V. V. Travnikov, A. Freiberg, and S. F. Savikhin, *J. Lumin.* **47**, 107 (1990).

<sup>9</sup>A. A. Bol, R. van Beek, and A. Meijerink, *Chem. Mater.* **14**, 1121 (2002).

<sup>10</sup>S. Y. Gao, H. J. Zhang, R. P. Deng, X. M. Wang, D. H. Sun, and G. L. Zheng, *Appl. Phys. Lett.* **89**, 123125 (2006).

<sup>11</sup>C. W. Chen, C. J. Pan, P. J. Huang, G. C. Chi, C. Y. Chang, F. Ren, and S. J. Pearton, *ECS Trans.* **16**, 13 (2008).

<sup>12</sup>L. Chen, J. Zhang, X. Zhang, F. Liu, and X. Wang, *Opt. Express* **16**, 11795 (2008).

<sup>13</sup>J. C. Ronfard-Haret, *J. Lumin.* **104**, 1 (2003).

<sup>14</sup>B. J. Pong, C. J. Pan, Y. C. Teng, G. C. Chi, W. H. Li, K. C. Lee, and C. H. Lee, *J. Appl. Phys.* **83**, 5992 (1998).

<sup>15</sup>J. W. Chiou, H. M. Tsai, C. W. Pao, F. Z. Chien, W. F. Pong, C. W. Chen, M.-H. Ysai, J. J. Wu, C. H. Ko, H. H. Chiang, H.-J. Lin, J. F. Lee, and J.-H. Guo, *J. Appl. Phys.* **104**, 013709 (2008).

<sup>16</sup>A. Goux, T. Pouporté, L. Robbiola, and D. Lincot, *Proc.-Electrochem. Soc.* **32**, 215 (2003).

<sup>17</sup>S. C. Ray, J. W. Chiou, W. F. Pong, and M. H. Tsai, *Crit. Rev. Solid State Mater. Sci.* **31**, 91 (2006).

<sup>18</sup>*Table of Periodic Properties of the Elements* (Sargent-Welch Scientific, Skokie, IL, 1980).

<sup>19</sup>J. W. Chiou, S. C. Ray, H. M. Tsai, C. W. Pao, F. Z. Chien, W. F. Pong, M. H. Tsai, J. J. Wu, C. H. Cheng, C. H. Chen, J. F. Lee, and J. H. Guo, *Appl. Phys. Lett.* **90**, 192112 (2007).

<sup>20</sup>M. Abdullah, T. Morimoto, and K. Okuyama, *Adv. Funct. Mater.* **13**, 800 (2003).